

Analysis of $VD_{s_0}^*D_{s1}$ and $VD_sD_s^*$ vertices

 R. Khosravi^{1,*} and M. Janbazi^{2,†}
¹*Department of Physics, Isfahan University of Technology, Isfahan 84156-83111, Iran*
²*Department of Physics, Shiraz Branch Islamic Azad University, Shiraz, Iran*

(Received 22 July 2013; published 7 January 2014)

The strong form factors and coupling constants of $VD_{s_0}^*D_{s1}$ and $VD_sD_s^*$ ($V = \phi, J/\psi$) vertices in the framework of the three-point QCD sum rules are considered. Taking into account the nonperturbative part contributions of the correlation functions, the quark-quark, gluon-gluon, and quark-gluon condensate as important terms are evaluated. Considering the $SU_f(3)$ symmetry, we compare our results with the values obtained in other methods.

DOI: 10.1103/PhysRevD.89.016001

PACS numbers: 11.55.Hx, 13.75.Lb, 12.38.Lg, 14.40.Lb

I. INTRODUCTION

There are various applications for the strong form factors and coupling constants associated with vertices that involve mesons in the QCD. To investigate meson interactions at high-energy physics, it is very important to know the exact functional form of the strong form factors in meson vertices. Therefore, they have received wide attention by researchers in the QCD.

Investigation of the strong form factors and coupling constants related to the charmed meson vertices is much more significant as it plays an important role in understanding the final state interactions in the QCD. In the production of charmonium J/ψ , $\psi(2s)$ and other cases that are useful sources of information in heavy ion collisions, there appear vertices involving charmed mesons, namely the $g_{DDJ/\psi}$, $g_{D^*DJ/\psi}$, and $g_{D^*D^*J/\psi}$ [1]. Also, the determination of strong coupling constants can provide a real possibility for studying the nature of the charmed pseudoscalar and axial vector mesons. For example, to recognize the structure of the new hadron states such as D_{s0} and D_{s1} , one can estimate the strong coupling constants for the $g_{D_{s0}DK}$ and $g_{D_{s1}D^*K}$ [2–4]. Until now, the vertices involving charmed mesons such as $D^*D^*\rho$ [5], $D^*D\pi$ [6,7], $DD\rho$ [8], $D^*D\rho$ [9], DDJ/ψ [10], D^*DJ/ψ [11], D^*D_sK , D_s^*DK , D_0D_sK , $D_{s0}DK$ [12], D^*D^*P , D^*DV , DDV [13], $D^*D^*\pi$ [14], D_sD^*K , D_s^*DK [15], $DD\omega$ [16], and D_sD_sV , $D_s^*D_s^*V$ [17] have been studied within the framework of the QCD sum rules.

The QCD sum rules have been successfully applied to a wide variety of problems in hadron physics [18] (for details of this method, see [19,20]). In this paper, we decide to calculate the strong form factors and coupling constants related to the $\phi D_{s_0}^*D_{s1}$, $\phi D_sD_s^*$, $J/\psi D_{s_0}^*D_{s1}$, and $J/\psi D_sD_s^*$ vertices via the three-point QCD sum rules (3PSR). To calculate the dependence of the form factors associated with each of these vertices on the transferred momentum

square Q^2 , we consider two cases: (1) when the charmed meson is an off-shell and (2) when the $\phi(J/\psi)$ meson is an off-shell. Understanding how to change the strong form factors in terms of Q^2 is essential to estimate the values of the coupling constants.

This paper includes three sections. In Sec. II, we present the QCD sum rules calculation for the strong form factors of the $\phi D_{s_0}^*D_{s1}$ vertex. In this way, we compute the quark-quark, gluon-quark, and gluon-gluon condensate contributions in the Borel transform scheme. These are the most important corrections of the nonperturbative part of the correlation function in the 3PSR method. Similarly, we can easily derive the strong form factors for the $\phi D_sD_s^*$, $J/\psi D_{s_0}^*D_{s1}$, and $J/\psi D_sD_s^*$ vertices. The next section depicts our numerical analysis of the strong form factors as well as the coupling constants with and without considering the $SU_f(3)$ symmetry. In this section, we also compare our results with values obtained in other approaches.

II. STRONG FORM FACTORS FOR THE $\phi D_{s_0}^*D_{s1}$ VERTEX VIA 3PSR

We start with the correlation function in the 3PSR to calculate the strong form factors associated with the $\phi D_{s_0}^*D_{s1}$ vertex. In this vertex, both strange charmed meson $D_{s_0}^*$ and ϕ can be an off-shell meson. For the off-shell $D_{s_0}^*$ meson [see Fig. 1(a)], the correlation function is given by

$$\begin{aligned} \Pi_{\mu\nu}^{D_{s_0}^*}(p, p') &= i^2 \int d^4x d^4y e^{i(p'x - py)} \\ &\times \langle 0 | \mathcal{T} \{ j_\mu^{D_{s_0}^*}(x) j_\nu^{D_{s_0}^* \dagger}(0) j_\nu^\phi(y) \} | 0 \rangle. \end{aligned} \quad (1)$$

For the off-shell ϕ meson [see Fig. 1(b)], this quantity is

$$\begin{aligned} \Pi_{\mu\nu}^\phi(p, p') &= i^2 \int d^4x d^4y e^{i(p'x - py)} \\ &\times \langle 0 | \mathcal{T} \{ j_\mu^{D_{s_0}^*}(x) j_\nu^\phi(0) j_\nu^{D_{s_0}^* \dagger}(y) \} | 0 \rangle, \end{aligned} \quad (2)$$

*rezakhosravi@cc.iut.ac.ir
†mehdijanbazi@yahoo.com

where $j^{D_{s0}^*} = \bar{s}c$, $j_{\mu}^{D_{s1}} = \bar{s}\gamma_{\mu}\gamma_5 c$, and $j_{\nu}^{\phi} = \bar{s}\gamma_{\nu}s$ are interpolating currents of the D_{s0}^* , D_{s1} , and ϕ mesons, respectively, and have the same quantum numbers as the associated mesons. Also, \mathcal{T} is the time-ordering product and p and p' are the four momentum of the initial and final mesons, respectively.

In the QCD sum rules approach, we can obtain the correlation functions of Eqs. (1) and (2) in two languages. The hadron language which is the physical or phenomenological side, and the quark-gluon language called the QCD or theoretical side. In the physical or phenomenological part, the representation is in terms of hadronic degrees of freedom which is responsible for the introduction of the form factors, decay constants, and masses. In the QCD or theoretical representation, we evaluate the correlation functions in terms of the QCD degrees of freedom like the quark-quark, gluon-gluon, and quark-gluon condensates, etc., using the Wilson operator product expansion (OPE).

In order to calculate the phenomenological parts of the correlation functions, three complete sets of intermediate states with the same quantum numbers as the currents $j_{\mu}^{D_{s1}}$, $j^{D_{s0}^*}$, and j_{ν}^{ϕ} should be inserted in Eqs. (1) and (2) as follows:

$$\begin{aligned}\Pi_{\mu\nu}^{D_{s0}^*} &= -\frac{\langle 0|j_{\mu}^{D_{s1}}|D_{s1}(p', \epsilon')\rangle\langle 0|j^{D_{s0}^*}|D_{s0}^*(q)\rangle\langle D_{s1}(p', \epsilon')|D_{s0}^*(q)\phi(p, \epsilon)\rangle\langle\phi(p, \epsilon)|j_{\nu}^{\phi}|0\rangle}{(p^2 - m_{\phi}^2)(p'^2 - m_{D_{s1}}^2)(q^2 - m_{D_{s0}^*}^2)} + \text{higher and continuum states,} \\ \Pi_{\mu\nu}^{\phi} &= -\frac{\langle 0|j_{\mu}^{D_{s1}}|D_{s1}(p', \epsilon')\rangle\langle 0|j^{D_{s0}^*}|D_{s0}^*(p)\rangle\langle D_{s1}(p', \epsilon')|D_{s0}^*(p)\phi(q, \epsilon)\rangle\langle\phi(q, \epsilon)|j_{\nu}^{\phi}|0\rangle}{(p^2 - m_{D_{s0}^*}^2)(p'^2 - m_{D_{s1}}^2)(q^2 - m_{\phi}^2)} + \text{higher and continuum states.}\end{aligned}\quad (3)$$

The matrix elements appearing in Eq. (3) are defined in the standard way in terms of strong form factor as well as the decay constants of the D_{s1} and ϕ meson as

$$\begin{aligned}\langle D_{s1}(p', \epsilon')|D_{s0}^*(q)\phi(p, \epsilon)\rangle &= ig_{\phi D_{s0}^* D_{s1}}(q^2)\epsilon^{\alpha\beta\sigma\gamma}\epsilon'_{\sigma}(p')\epsilon_{\gamma}(p)p_{\alpha}p'_{\beta}, & \langle 0|j^{D_{s0}^*}|D_{s0}^*\rangle &= m_{D_{s0}^*}f_{D_{s0}^*}, \\ \langle 0|j_{\mu}^{D_{s1}}|D_{s1}\rangle &= m_{D_{s1}}f_{D_{s1}}\epsilon'_{\mu}, & \langle 0|j_{\nu}^{\phi}|\phi\rangle &= m_{\phi}f_{\phi}\epsilon_{\nu},\end{aligned}\quad (4)$$

where $q = p' - p$, $g_{\phi D_{s0}^* D_{s1}}(q^2)$ is the strong form factor, $m_{D_{s0}^*}$, $m_{D_{s1}}$, m_{ϕ} , and $f_{D_{s0}^*}$, $f_{D_{s1}}$, f_{ϕ} are the masses and the decay constants of the D_{s0}^* , D_{s1} , ϕ mesons, respectively. Also, ϵ and ϵ' are the polarization of the ϕ and D_{s1} meson, respectively.

Using Eq. (4) in Eq. (3) and after some calculations, we obtain

$$\begin{aligned}\Pi_{\mu\nu}^{D_{s0}^*} &= -g_{\phi D_{s0}^* D_{s1}}^{D_{s0}^*}(q^2)\frac{m_{D_{s1}}m_{D_{s0}^*}m_{\phi}f_{D_{s1}}f_{D_{s0}^*}f_{\phi}}{(q^2 - m_{D_{s0}^*}^2)(p^2 - m_{\phi}^2)(p'^2 - m_{D_{s1}}^2)}i\epsilon^{\alpha\beta\mu\nu}p_{\alpha}p'_{\beta} + \text{higher and continuum states,} \\ \Pi_{\mu\nu}^{\phi} &= -g_{\phi D_{s0}^* D_{s1}}^{\phi}(q^2)\frac{m_{D_{s1}}m_{D_{s0}^*}m_{\phi}f_{D_{s1}}f_{D_{s0}^*}f_{\phi}}{(q^2 - m_{\phi}^2)(p^2 - m_{D_{s0}^*}^2)(p'^2 - m_{D_{s1}}^2)}i\epsilon^{\alpha\beta\mu\nu}p_{\alpha}p'_{\beta} + \text{higher and continuum states.}\end{aligned}\quad (5)$$

Now, we calculate the QCD side of the correlation functions for the $\phi D_{s0}^* D_{s1}$ vertex. To this aim, the correlation functions containing the perturbative and nonperturbative parts are written as follows:

$$\Pi_{\mu\nu}^{D_{s0}^*(\phi)} = (\Pi_{\text{per}}^{D_{s0}^*(\phi)} + \Pi_{\text{nonper}}^{D_{s0}^*(\phi)})i\epsilon^{\alpha\beta\mu\nu}p_{\alpha}p'_{\beta} + \text{other structures and the higher states.}\quad (6)$$

Using the double dispersion relation for the coefficient of the Lorentz structure $i\epsilon^{\alpha\beta\mu\nu}p_{\alpha}p'_{\beta}$, which appears in the correlation functions [Eq. (6)], we calculate the perturbative part as

$$\Pi_{\text{per}}^{D_{s0}^*(\phi)} = -\frac{1}{4\pi^2}\int ds\int ds'\frac{\rho^{D_{s0}^*(\phi)}}{(s-p^2)(s'-p'^2)} + \text{subtraction terms,}\quad (7)$$

where $\rho^{D_{s0}^*(\phi)}$ is the spectral density. We calculate the spectral densities in terms of the usual Feynman integrals by the help of the Cutkosky rules, where the quark propagators are replaced by Dirac-delta functions, i.e., $\frac{1}{p^2 - m^2} \rightarrow (-2\pi i)\delta(p^2 - m^2)$.

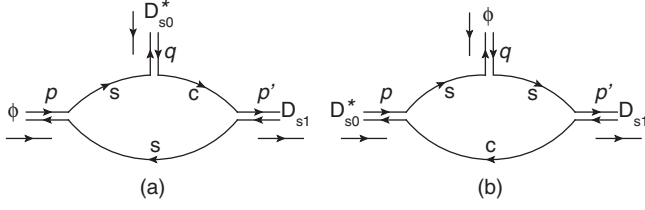


FIG. 1. Perturbative diagrams for the off-shell $D_{s_0}^*$ (a) and the off-shell ϕ meson (b).

Figure 1 shows the perturbative loop diagrams for the $\phi D_{s_0}^* D_{s_1}$ vertex. Using Fig. 1 and after some straightforward calculations for the structure $i\varepsilon^{\alpha\beta\mu\nu} p_\alpha p'_\beta$, we have

$$\begin{aligned} \rho_{\phi D_{s_0}^* D_{s_1}}^{D_{s_0}^*}(s, s', q^2) &= \frac{3}{\sqrt{\lambda}} [\lambda B_1 (m_c + m_s) + m_s], \\ \rho_{\phi D_{s_0}^* D_{s_1}}^\phi(s, s', q^2) &= -\frac{3}{\sqrt{\lambda}} [\lambda B_2 (m_s + m_c) + m_c], \end{aligned} \quad (8)$$

where

$$\begin{aligned} B_1 &= s(s' - s + 2m_s^2 - 2m_c^2 + q^2), \\ B_2 &= (s + s' + 2m_c^2 - 2m_s^2)q^2 - (s - s')^2, \\ \lambda &= (s + s' - q^2)^2 - 4ss'. \end{aligned} \quad (9)$$

After calculating the perturbative part, we are going to calculate the nonperturbative part of the correlation functions. In the QCD, the three-point correlation functions can be expanded by the OPE in the deep Euclidean region, where $p^2, p'^2 \rightarrow -\infty$, in terms of a series of local operators. Taking into account the vacuum expectation value of the OPE, the correlation functions in terms of local operators with the increasing dimension are written as follows,

$$\begin{aligned} \Pi^{D_{s_0}^*(\phi)} &= C_0^{D_{s_0}^*(\phi)} + C_3^{D_{s_0}^*(\phi)} \langle \bar{q}q \rangle + C_4^{D_{s_0}^*(\phi)} \langle G_{\alpha\beta}^a G^{a\alpha\beta} \rangle \\ &+ C_5^{D_{s_0}^*(\phi)} \langle \bar{q} \sigma_{\alpha\beta} T^a G^{a\alpha\beta} q \rangle + C_6^{D_{s_0}^*(\phi)} \langle \bar{q} \Gamma q \bar{q} \Gamma' q \rangle \\ &+ \dots, \end{aligned} \quad (10)$$

where C_i are the Wilson coefficients, $G_{\alpha\beta}^a$ is the gluon field strength tensor, and Γ and Γ' are the matrices

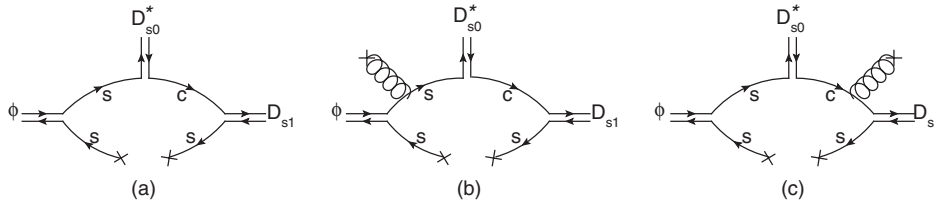


FIG. 2. Nonperturbative diagrams for the off-shell ϕ meson in the $\phi D_{s_0}^* D_{s_1}$ vertex.

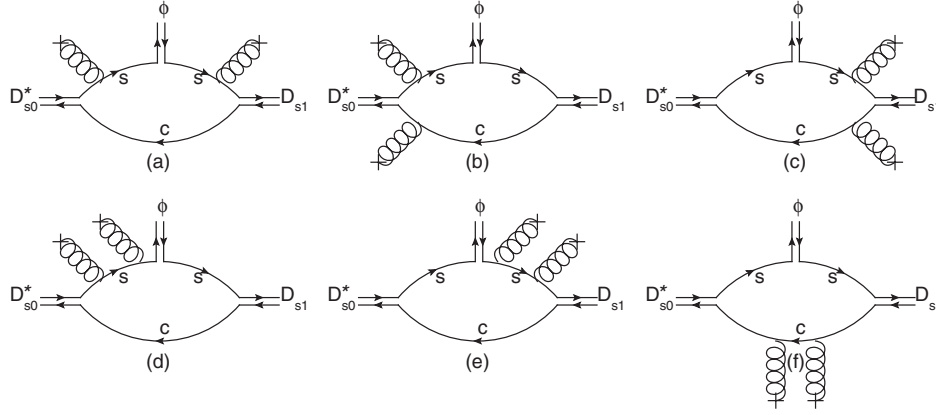
appearing in the calculations. In Eq. (10), C_0 is related to the contribution of the perturbative part of the correlation functions and other terms are related to the nonperturbative contributions of them. The important condensate terms of dimensions three, four, and five are related to the contributions of the quark-quark, gluon-gluon and quark-gluon condensates, respectively. The perturbative part contribution of the correlation functions was discussed before. For the calculation of the nonperturbative contributions, we only consider the important condensate terms in each case. When the $D_{s_0}^*$ meson is an off-shell, the gluon-gluon condensate contributions can be easily ignored. Therefore, important diagrams of dimensions three and five result from the nonperturbative part contributions. These diagrams are depicted in Fig. 2. On the other hand, when the ϕ is an off-shell meson, the quark-quark, and quark-gluon condensate contributions are suppressed and the most important contribution of the nonperturbative part comes from the gluon-gluon diagrams. Figure 3 shows these diagrams that are related to the gluon-gluon condensate.

After some complicated calculations, we have obtained the results for the important nonperturbative contributions by applying the double Borel transformations as $C_{\phi D_{s_0}^* D_{s_1}}^{D_{s_0}^*}$ and $C_{\phi D_{s_0}^* D_{s_1}}^\phi$ for the off-shell $D_{s_0}^*$ and ϕ meson, respectively. The explicit expressions of the $C_{\phi D_{s_0}^* D_{s_1}}^{D_{s_0}^*}$ and $C_{\phi D_{s_0}^* D_{s_1}}^\phi$ are given in the Appendix. It should be noted that to obtain the gluon condensate contributions, we follow the same procedure as stated in [21].

The QCD sum rules for the strong form factors are obtained by equating two representations of the correlation functions and applying the double Borel transformation with respect to the p^2 and p'^2 as

$$\begin{aligned} B_{p^2}(M_1^2) \left(\frac{1}{p^2 - m^2} \right)^n &= \frac{(-1)^n e^{-m^2/M_1^2}}{\Gamma(n) (M_1^2)^n}, \\ B_{p'^2}(M_2^2) \left(\frac{1}{p'^2 - m^2} \right)^n &= \frac{(-1)^n e^{-m^2/M_2^2}}{\Gamma(n) (M_2^2)^n}, \end{aligned}$$

on the phenomenological as well as the perturbative and nonperturbative parts of the correlation functions in order to suppress the contributions of the higher states and continuum. We obtain the equations for the strong form factors as follows,

FIG. 3. Nonperturbative diagrams for the off-shell D_{s0}^* meson in the $\phi D_{s0}^* D_{s1}$ vertex.

$$\begin{aligned}
 g_{\phi D_{s0}^* D_{s1}}^{D_{s0}^*}(Q^2) &= -\frac{(Q^2 + m_{D_{s0}^*}^2)}{m_\phi m_{D_{s1}} m_{D_{s0}^*} f_\phi f_{D_{s1}} f_{D_{s0}^*}} e^{\frac{m_\phi^2}{M_1^2}} e^{\frac{m_{D_{s1}}^2}{M_2^2}} \left\{ -\frac{1}{4\pi^2} \int_{(m_c+m_s)^2}^{s_0^{D_{s1}}} ds' \int_{s_1}^{s_0^\phi} ds \rho_{\phi D_{s0}^* D_{s1}}^{D_{s0}^*}(s, s', Q^2) e^{-\frac{s}{M_1^2}} e^{-\frac{s'}{M_2^2}} + M_1^2 M_2^2 C_{\phi D_{s0}^* D_{s1}}^{D_{s0}^*} \right\}, \\
 g_{\phi D_{s0}^* D_{s1}}^\phi(Q^2) &= -\frac{(Q^2 + m_\phi^2)}{m_\phi m_{D_{s1}} m_{D_{s0}^*} f_\phi f_{D_{s1}} f_{D_{s0}^*}} \\
 &\quad \times e^{\frac{m_{D_{s0}^*}^2}{M_1^2}} e^{\frac{m_{D_{s1}}^2}{M_2^2}} \left\{ -\frac{1}{4\pi^2} \int_{(m_c+m_s)^2}^{s_0^{D_{s1}}} ds' \int_{s_2}^{s_0^{D_{s0}^*}} ds \rho_{\phi D_{s0}^* D_{s1}}^\phi(s, s', Q^2) e^{-\frac{s}{M_1^2}} e^{-\frac{s'}{M_2^2}} + M_1^2 M_2^2 C_{\phi D_{s0}^* D_{s1}}^\phi \right\}, \quad (11)
 \end{aligned}$$

where $Q^2 = -q^2$, $s_0^{D_{s1}}$, $s_0^{D_{s0}^*}$, and s_0^ϕ are the continuum thresholds of the D_{s1} , D_{s0}^* , and ϕ mesons, respectively. s_1 and s_2 are the lower limits of the integrals over s as

$$s_1 = \frac{(s' - q^2)(m_s^2 s' - q^2 m_c^2)}{(m_s^2 - q^2)(m_c^2 - s')}, \quad s_2 = \frac{(m_c^2 + q^2 - m_s^2 - s')(m_s^2 s' - q^2 m_c^2)}{(m_s^2 - q^2)(m_c^2 - s')}.$$

Repeating the same steps as done before but for the $\phi D_s D_s^*$ vertex within the 3PSR method, we can easily evaluate the related strong form factors as

$$\begin{aligned}
 g_{\phi D_s D_s^*}^{D_s}(Q^2) &= -\frac{(m_c + m_s)(Q^2 + m_{D_s}^2)}{m_\phi m_{D_s^*} m_{D_s}^2 f_\phi f_{D_s^*} f_{D_s}} e^{\frac{m_\phi^2}{M_1^2}} e^{\frac{m_{D_s^*}^2}{M_2^2}} \left\{ -\frac{1}{4\pi^2} \int_{(m_c+m_s)^2}^{s_0^{D_s^*}} ds' \int_{s_1}^{s_0^\phi} ds \rho_{\phi D_s D_s^*}^{D_s}(s, s', Q^2) e^{-\frac{s}{M_1^2}} e^{-\frac{s'}{M_2^2}} + M_1^2 M_2^2 C_{\phi D_s D_s^*}^{D_s} \right\}, \\
 g_{\phi D_s D_s^*}^\phi(Q^2) &= -\frac{(m_c + m_s)(Q^2 + m_\phi^2)}{m_\phi m_{D_s^*} m_{D_s}^2 f_\phi f_{D_s^*} f_{D_s}} e^{\frac{m_{D_s}^2}{M_1^2}} e^{\frac{m_{D_s^*}^2}{M_2^2}} \left\{ -\frac{1}{4\pi^2} \int_{(m_c+m_s)^2}^{s_0^{D_s^*}} ds' \int_{s_2}^{s_0^{D_s}} ds \rho_{\phi D_s D_s^*}^\phi(s, s', Q^2) e^{-\frac{s}{M_1^2}} e^{-\frac{s'}{M_2^2}} + M_1^2 M_2^2 C_{\phi D_s D_s^*}^\phi \right\}, \quad (12)
 \end{aligned}$$

where

$$\rho_{\phi D_s D_s^*}^{D_s}(s, s', q^2) = \frac{3}{\sqrt{\lambda}} [\lambda B_1 (m_c - m_s) - m_s], \quad \rho_{\phi D_s D_s^*}^\phi(s, s', q^2) = -\frac{3}{\sqrt{\lambda}} [\lambda B_2 (m_s - m_c) - m_c].$$

Also, the expressions of the coefficients $C_{\phi D_s D_s^*}^{D_s}$ and $C_{\phi D_s D_s^*}^\phi$ are given in the Appendix.

Finally, we would like to provide the same results for the $J/\psi D_{s0}^* D_{s1}$ and $J/\psi D_s D_s^*$ vertices. With a little bit of change in the above expressions, such as the change in the quark permutations, we can easily find similar results in Eqs. (11) and (12) for the strong form factors of the new vertices as

$$\begin{aligned}
g_{J/\psi D_{s0}^* D_{s1}}^{D_{s0}^*}(Q^2) &= -\frac{(Q^2 + m_{D_{s0}^*}^2)}{m_{J/\psi} m_{D_{s1}} m_{D_{s0}^*} f_{J/\psi} f_{D_{s1}} f_{D_{s0}^*}} \\
&\times e^{\frac{m_{J/\psi}^2}{M_1^2} e^{\frac{m_{D_{s1}}^2}{M_2^2}}} \left\{ -\frac{1}{4\pi^2} \int_{(m_c+m_s)^2}^{s_0^{D_{s1}}} ds' \int_{s_1'}^{s_0^{J/\psi}} ds \rho_{J/\psi D_{s0}^* D_{s1}}^{D_{s0}^*}(s, s', Q^2) e^{-\frac{s}{M_1^2} e^{-\frac{s'}{M_2^2}} + M_1^2 M_2^2 C_{J/\psi D_{s0}^* D_{s1}}^{D_{s0}^*}} \right\}, \\
g_{J/\psi D_{s0}^* D_{s1}}^{J/\psi}(Q^2) &= -\frac{(Q^2 + m_{J/\psi}^2)}{m_{J/\psi} m_{D_{s1}} m_{D_{s0}^*} f_{J/\psi} f_{D_{s1}} f_{D_{s0}^*}} \\
&\times e^{\frac{m_{D_{s0}^*}^2}{M_1^2} e^{\frac{m_{D_{s1}}^2}{M_2^2}}} \left\{ -\frac{1}{4\pi^2} \int_{(m_c+m_s)^2}^{s_0^{D_{s1}}} ds' \int_{s_2'}^{s_0^{D_{s0}^*}} ds \rho_{J/\psi D_{s0}^* D_{s1}}^{J/\psi}(s, s', Q^2) e^{-\frac{s}{M_1^2} e^{-\frac{s'}{M_2^2}} + M_1^2 M_2^2 C_{J/\psi D_{s0}^* D_{s1}}^{J/\psi}} \right\}, \\
g_{J/\psi D_s D_s^*}^{D_s}(Q^2) &= -\frac{(m_c + m_s)(Q^2 + m_{D_s}^2)}{m_{J/\psi} m_{D_s} m_{D_s}^2 f_{J/\psi} f_{D_s}^* f_{D_s}} \\
&\times e^{\frac{m_{J/\psi}^2}{M_1^2} e^{\frac{m_{D_s}^2}{M_2^2}}} \left\{ -\frac{1}{4\pi^2} \int_{(m_c+m_s)^2}^{s_0^{D_s}} ds' \int_{s_1'}^{s_0^{J/\psi}} ds \rho_{J/\psi D_s D_s^*}^{D_s}(s, s', Q^2) e^{-\frac{s}{M_1^2} e^{-\frac{s'}{M_2^2}} + M_1^2 M_2^2 C_{J/\psi D_s D_s^*}^{D_s}} \right\}, \\
g_{J/\psi D_s D_s^*}^{J/\psi}(Q^2) &= -\frac{(m_c + m_s)(Q^2 + m_{J/\psi}^2)}{m_{J/\psi} m_{D_s} m_{D_s}^2 f_{J/\psi} f_{D_s}^* f_{D_s}} \\
&\times e^{\frac{m_{D_s}^2}{M_1^2} e^{\frac{m_{D_s}^2}{M_2^2}}} \left\{ -\frac{1}{4\pi^2} \int_{(m_c+m_s)^2}^{s_0^{D_s}} ds' \int_{s_2'}^{s_0^{D_s}} ds \rho_{J/\psi D_s D_s^*}^{J/\psi}(s, s', Q^2) e^{-\frac{s}{M_1^2} e^{-\frac{s'}{M_2^2}} + M_1^2 M_2^2 C_{J/\psi D_s D_s^*}^{J/\psi}} \right\},
\end{aligned}$$

where

$$\begin{aligned}
\rho_{J/\psi D_{s0}^* D_{s1}}^{D_{s0}^*} &= \rho_{\phi D_{s0}^* D_{s1}}^{D_{s0}^*} |_{s \leftrightarrow c}, & C_{J/\psi D_{s0}^* D_{s1}}^{D_{s0}^*} &= -C_{\phi D_{s0}^* D_{s1}}^{\phi} |_{s \leftrightarrow c}, \\
\rho_{J/\psi D_{s0}^* D_{s1}}^{J/\psi} &= \rho_{\phi D_{s0}^* D_{s1}}^{\phi} |_{s \leftrightarrow c}, & C_{J/\psi D_{s0}^* D_{s1}}^{J/\psi} &= -C_{\phi D_{s0}^* D_{s1}}^{D_{s0}^*} |_{s \leftrightarrow c}, \\
\rho_{J/\psi D_s D_s^*}^{D_s} &= \rho_{\phi D_s D_s^*}^{D_s} |_{s \leftrightarrow c}, & C_{J/\psi D_s D_s^*}^{D_s} &= -C_{\phi D_s D_s^*}^{\phi} |_{s \leftrightarrow c}, \\
\rho_{J/\psi D_s D_s^*}^{J/\psi} &= \rho_{\phi D_s D_s^*}^{\phi} |_{s \leftrightarrow c}, & C_{J/\psi D_s D_s^*}^{J/\psi} &= -C_{\phi D_s D_s^*}^{D_s} |_{s \leftrightarrow c}, \\
s_1' &= s_1 |_{s \leftrightarrow c}, & s_2' &= s_2 |_{s \leftrightarrow c}.
\end{aligned}$$

III. NUMERICAL ANALYSIS

In this section, the strong form factors and coupling constants for the $VD_{s0}^*D_{s1}$ and $VD_sD_s^*$ ($V = \phi, J/\psi$) vertices are analyzed. We choose the values of meson and quark masses as $m_\phi = 1.020$, $m_{J/\psi} = 3.097$, $m_{D_{s0}^*} = 2.318$, $m_{D_s} = 1.969$, $m_{D_s^*} = 2.112$, $m_{D_{s1}} = 2.460$, $m_s = 0.104$ GeV [22]. Also, the leptonic decay constants used in this calculation are taken as $f_\phi = 0.234$ [23], $f_{J/\psi} = 0.405$ [1], $f_{D_{s0}^*} = 0.225$ [24], $f_{D_s} = 0.274$ [25], $f_{D_s^*} = 0.266$ [24], and $f_{D_{s1}} = 0.240$ GeV [26]. For a comprehensive analysis,

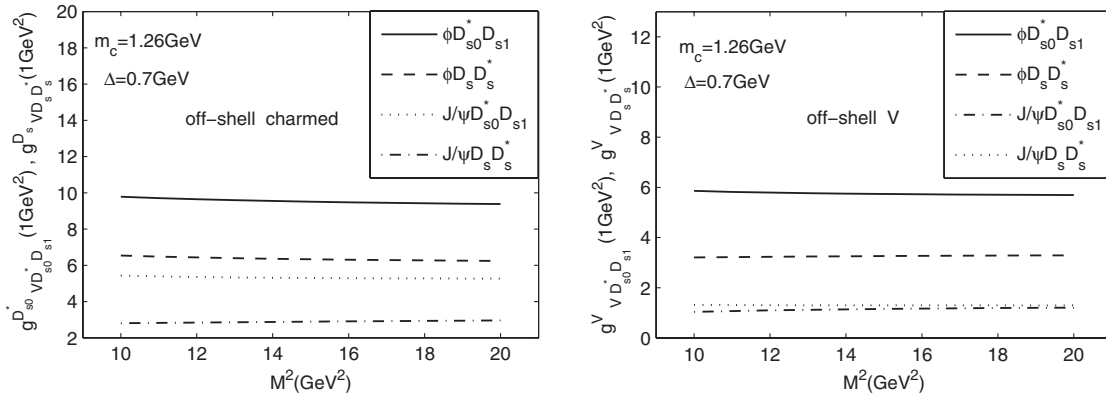


FIG. 4. The strong form factors, $g_{VD_{s0}^* D_{s1}}^{D_{s0}^*}$, $g_{VD_s D_s^*}^{D_s}$, $g_{VD_{s0}^* D_{s1}}^{J/\psi}$, and $g_{VD_s D_s^*}^{J/\psi}$, as functions of the Borel mass parameter, M^2 in $Q^2 = 1$ GeV², for the off-shell charmed mesons (left) and the off-shell V meson (right).

TABLE I. Parameters appearing in the fit functions for the strong form factors in two sets and various data of Δ , where $\Delta_1 = 0.4$, $\Delta_2 = 0.7$, and $\Delta_3 = 1.0$ GeV.

Form factor	Set I				Set II			
	$A(\Delta_1)$	$B(\Delta_1)$	$A(\Delta_2)$	$B(\Delta_2)$	$A(\Delta_3)$	$B(\Delta_3)$	$A(\Delta_2)$	$B(\Delta_2)$
$g_{\phi D_{s0}^* D_{s1}}^{D_{s0}^*}$	210.54	31.78	337.21	45.61	372.46	47.12	312.03	42.67
$g_{\phi D_{s0}^* D_{s1}}^{\phi}$	7.13	53.60	7.78	89.44	8.76	229.10	7.06	18.52
$g_{\phi D_s D_s^*}^{D_s}$	84.10	25.21	85.57	21.55	88.87	19.26	81.39	17.58
$g_{\phi D_s D_s^*}^{\phi}$	2.91	11.82	3.70	12.57	4.45	17.73	3.97	7.88
$g_{J/\psi D_{s0}^* D_{s1}}^{D_{s0}^*}$	144.50	29.32	247.46	42.71	519.19	77.80	59.47	17.06
$g_{J/\psi D_{s0}^* D_{s1}}^{J/\psi}$	2.48	11.48	3.07	13.24	3.78	15.78	3.44	28.85
$g_{J/\psi D_s D_s^*}^{D_s}$	72.30	29.90	166.79	52.07	689.76	178.27	37.39	15.29
$g_{J/\psi D_s D_s^*}^{J/\psi}$	2.38	729.62	3.01	208.99	3.57	135.55	2.87	314.21

we use the value of the c quark mass in two sets: set I, $m_c = 1.26$ GeV, and set II, $m_c = 1.47$ GeV.

In the 3PSR calculations, the expressions for the strong form factors also contain mathematical parameters, M_1^2 and M_2^2 , and continuum thresholds, s_0^m ($m = \phi, J/\psi, D_{s0}^*, D_s, D_s^*, D_{s1}$). These are mathematical objects, so the physical quantities i.e., strong form factors and coupling constants, should be independent of them. The values of the continuum thresholds are taken to be $s_0^m = (m_m + \Delta)^2$, where m_m is the meson mass. We use $0.4 \text{ GeV} \leq \Delta \leq 1 \text{ GeV}$ [27]. The working regions for the M_1^2 and M_2^2 are determined by requiring not only that the contributions of the higher states and continuum be effectively suppressed, but also that the contributions of the higher-dimensional operators are small. In this work, we use the following relation between the Borel mass parameters, M_1^2 and M_2^2 [5,10],

$$\frac{M_1^2}{M_2^2} = \frac{m_i^2}{m_o^2}, \quad (13)$$

where m_i and m_o are the masses of the incoming and outgoing meson, respectively. According to this relation between the

M_1^2 and M_2^2 , we will have only one independent the Borel mass parameter, M^2 . We found a good stability for the sum rules in the interval $10 \text{ GeV}^2 \leq M^2 \leq 20 \text{ GeV}^2$, in all vertices. The dependence of the strong form factors $g_{V D_{s0}^* D_{s1}}^{D_{s0}^*}$, $g_{V D_s D_s^*}^{D_s}$, $g_{V D_{s0}^* D_{s1}}^{\phi}$, and $g_{V D_s D_s^*}^{\phi}$ on the Borel mass parameter, M^2 in $Q^2 = 1 \text{ GeV}^2$, $m_c = 1.26 \text{ GeV}$, and $\Delta = 0.7 \text{ GeV}$ is shown in Fig. 4.

Equation (11) shows the Q^2 dependence of the strong form factors in the region where the sum rule is valid. To extend these results to the full region, we look for parametrization of the form factors in such that in the validity region of the 3PSR, this parametrization coincides with the sum rules prediction. For the off-shell charmed mesons, our numerical calculations show that the sufficient parametrization of the form factors with respect to Q^2 is (Monopole fit function)

$$g(Q^2) = \frac{A}{Q^2 + B}, \quad (14)$$

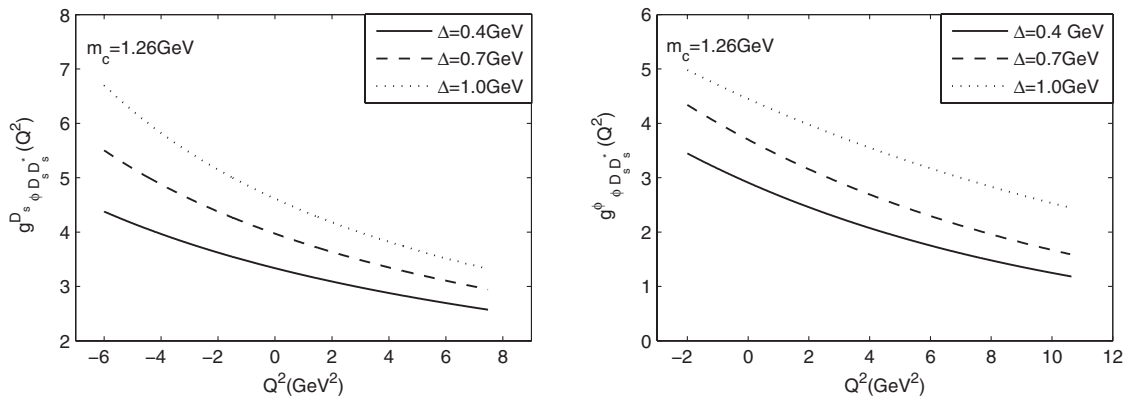


FIG. 5. The strong form factor, $g_{\phi D_s D_s^*}$ on Q^2 , in the different values of Δ , for the off-shell D_s meson (left) and the off-shell ϕ meson (right).

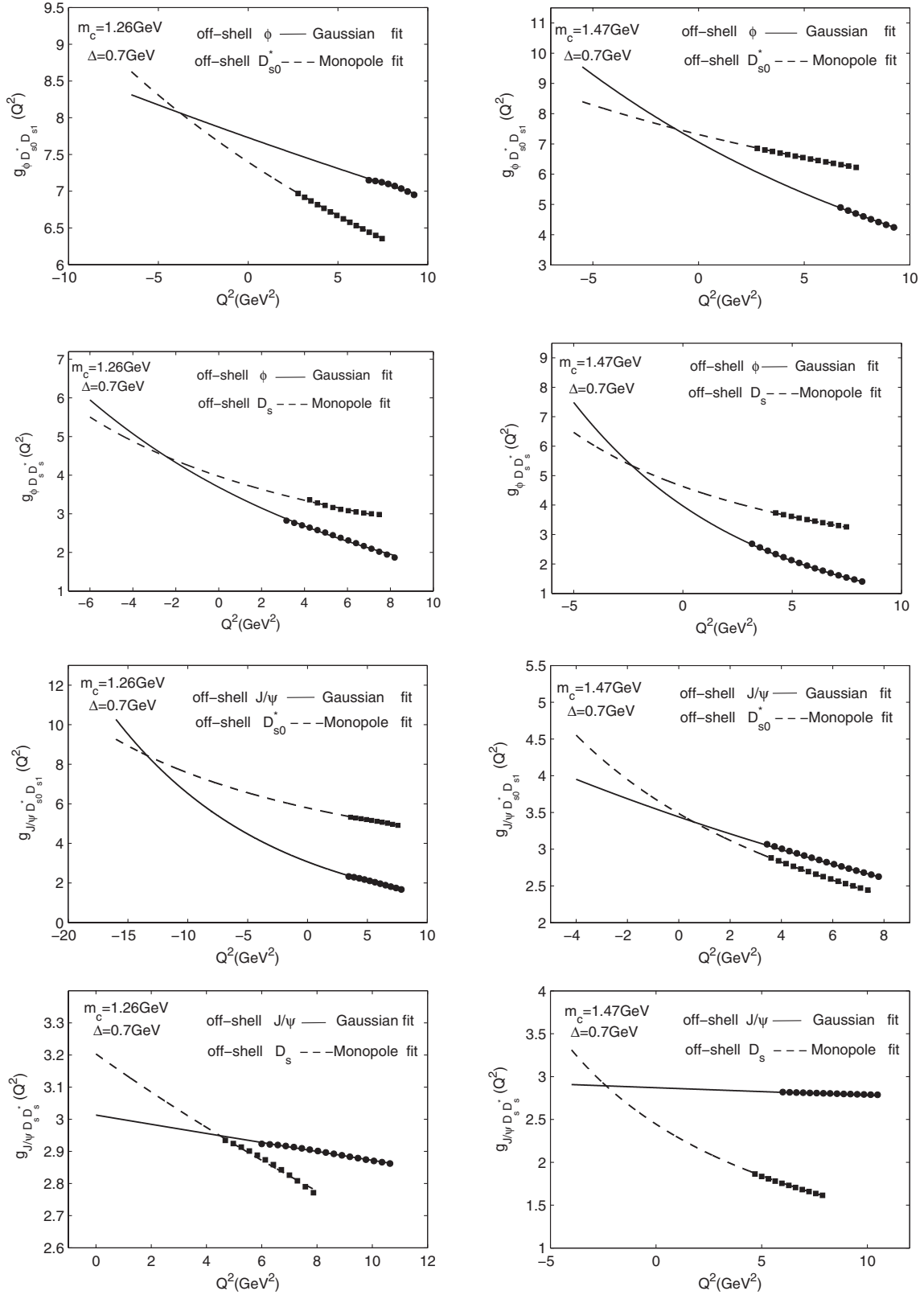


FIG. 6. The strong form factors of each vertex on Q^2 for $\Delta = 0.7$ and different values of m_c for the off-shell $\phi(J/\psi)$ and charmed mesons.

TABLE II. The strong coupling constants in GeV^{-1} for different values of m_c .

Coupling constant	Set I		Set II	
	Off-shell charmed	Off-shell ϕ	Off-shell charmed	Off-shell ϕ
$g_{\phi D_{s0}^* D_{s1}}$	8.38 ± 0.54	8.03 ± 0.79	8.36 ± 0.53	8.22 ± 0.83
$g_{\phi D_s D_s^*}$	4.86 ± 0.93	4.63 ± 0.69	5.94 ± 1.03	5.68 ± 0.89
$g_{J/\psi D_{s0}^* D_{s1}}$	6.63 ± 0.59	6.34 ± 0.63	5.09 ± 0.48	4.80 ± 0.45
$g_{J/\psi D_s D_s^*}$	3.46 ± 0.59	3.15 ± 0.74	3.27 ± 0.55	2.90 ± 0.64

TABLE III. Parameters appearing in the fit functions for the form factors in $SU_f(3)$ symmetry, $m_c = 1.26$ and $\Delta = 0.7$ GeV.

Form factor	A	B	Form factor	A	B
$g_{\phi D_{s0}^* D_{s1}}^{D_{s0}^*}$	432.41	51.01	$g_{J/\psi D_{s0}^* D_{s1}}^{D_{s0}^*}$	209.20	41.09
$g_{\phi D_{s0}^* D_{s1}}^{\phi}$	9.22	44.90	$g_{J/\psi D_{s0}^* D_{s1}}^{J/\psi}$	3.68	22.53
$g_{\phi D_s D_s^*}^{D_s}$	26.10	10.07	$g_{J/\psi D_s D_s^*}^{D_s}$	89.61	32.55
$g_{\phi D_s D_s^*}^{\phi}$	3.08	11.55	$g_{J/\psi D_s D_s^*}^{J/\psi}$	2.58	74.59

TABLE IV. The strong coupling constants in GeV^{-1} in $SU_f(3)$ symmetry for $m_c = 1.26$ GeV.

Coupling constant	Off-shell charmed	Off-shell ϕ	Off-shell J/ψ
$g_{\phi D_{s0}^* D_{s1}}$	9.47 ± 0.60	9.82 ± 0.85	...
$g_{\phi D_s D_s^*}$	4.21 ± 0.82	3.93 ± 0.62	...
$g_{J/\psi D_{s0}^* D_{s1}}$	5.86 ± 0.68	...	5.64 ± 0.71
$g_{J/\psi D_s D_s^*}$	3.12 ± 0.60	...	2.93 ± 0.63

and for the off-shell V meson, the strong form factors can be fitted by the exponential fit function as given (Gaussian fit function),

$$g(Q^2) = A e^{-Q^2/B}. \quad (15)$$

The values of the parameters A and B for the strong form factors of the $VD_{s0}^* D_{s1}$ and $VD_s D_s^*$ vertices in two sets and various data of Δ are given in Table I.

Figure 5 shows variation of the strong form factors, $g_{\phi D_s D_s^*}^{D_s}$ and $g_{\phi D_s D_s^*}^{\phi}$, for different amounts of $A(\Delta)$ and $B(\Delta)$.

The Q^2 dependence of the strong form factors in two sets and $\Delta = 0.7$ is shown in Fig. 6. In this figure, the small circles and boxes correspond to the form factors via the 3PSR calculations. As can be seen, the form factors and

their fit functions coincide, well. Figure 6 clearly shows intersection point of the two diagrams, for the off-shell $\phi(J/\psi)$ and the off-shell charmed mesons in each plot.

The coupling constant as the value of the strong form factor is defined at $Q^2 = -m_m^2$ in Eqs. (14) and (15), where m_m is the mass of the off-shell meson. Considering the uncertainties in the values of other input parameters, we obtain the values of the strong coupling constants in two sets shown in Table II.

For a better analysis, we want to consider the strong coupling constants with the $SU_f(3)$ symmetry. In the $SU_f(3)$ symmetry, the s quark mass is equal to the mass of light quarks. Considering the $SU_f(3)$ symmetry, the values of parameters A and B for the fit form factors of the $\phi D_{s0}^* D_{s1}$, $\phi D_s D_s^*$, $J/\psi D_{s0}^* D_{s1}$, and $J/\psi D_s D_s^*$ vertices in $m_c = 1.26$ and $\Delta = 0.7$ GeV can be obtained as given in Table III. In Table IV, we present the values of the strong coupling constants of the $\phi D_{s0}^* D_{s1}$, $\phi D_s D_s^*$, $J/\psi D_{s0}^* D_{s1}$, and $J/\psi D_s D_s^*$ vertices via the $SU_f(3)$ symmetry.

Finally, we would like to compare our results with the values predicted by other methods. Taking an average of the two values of the coupling constant for the $g_{\phi D_s D_s^*}$, as presented in Table III, we obtain 4.07 ± 0.71 GeV^{-1} . Also, the value of the same quantity for the $g_{J/\psi D_s D_s^*}$ is 3.03 ± 0.62 GeV^{-1} .

In the $SU_f(3)$ symmetry, the coupling constant values for the $g_{\rho DD^*}$ and $g_{J/\psi DD^*}$ are nearly equal to those for the $g_{\phi D_s D_s^*}$ and $g_{J/\psi D_s D_s^*}$, respectively. This means that we have

$$g_{\rho DD^*} \approx g_{\phi D_s D_s^*} = 4.07 \pm 0.71 \text{ GeV}^{-1},$$

$$g_{J/\psi DD^*} \approx g_{J/\psi D_s D_s^*} = 3.03 \pm 0.62 \text{ GeV}^{-1}. \quad (16)$$

In Table V, we compare our results with those of other approaches such as the 3PSR, the vector meson dominance (VMD), the light-cone QCD sum rules (LCSR), and the quark model (QM).

It should be noted that in our calculation, the main contribution comes from the perturbative part of the strong form factors and the contribution of the nonperturbative part containing the quark-quark and quark-gluon diagrams in Fig. 2, which is about 20% of the total and the gluon-gluon contribution in Fig. 3 is about 10%.

The errors in our evaluations are estimated by the variation of the Borel parameter M^2 , the variation of the continuum thresholds, and the leptonic decay constants and uncertainties in the values of other input parameters. The main uncertainty comes from the continuum thresholds and the decay constants.

TABLE V. The values of the strong coupling constants for $g_{\rho DD^*}$ and $g_{J/\psi DD^*}$ via different approaches: 3PSR, VMD, LCSR, and QM.

Coupling constant	Our	3PSR	VMD	LCSR	QM
$g_{\rho DD^*}$	4.07 ± 0.71	4.11[9]	2.82[28]	3.56[12], 4.17[29]	...
$g_{J/\psi DD^*}$	3.03 ± 0.62	3.48[11]	4.05[30]	...	8.02[31]

To summarize, by considering the contributions of the quark-quark, quark-gluon, and gluon-gluon condensate corrections, we estimated the strong form factors for the $\phi D_{s0}^*D_{s1}$, $\phi D_sD_s^*$, $J/\psi D_{s0}^*D_{s1}$, and $J/\psi D_sD_s^*$ vertices within the 3PSR. The dependence of the strong form factors on the transferred momentum square Q^2 was plotted. We also evaluated the coupling constants of these vertices. Detection of these strong form factors and the coupling constants and their comparison with the phenomenological models like the QCD sum rules could give useful information about strong interactions of the strange charmed mesons.

ACKNOWLEDGMENTS

Partial support of the Isfahan University of Technology Research Council is appreciated.

APPENDIX

In this appendix, the explicit expressions of the coefficients $C_{\phi D_{s0}^*D_{s1}}^{D_{s0}^*}$, $C_{\phi D_sD_s^*}^{D_s}$, $C_{\phi D_{s0}^*D_{s1}}^\phi$, and $C_{\phi D_sD_s^*}^\phi$ are given by applying the double Borel transformations,

$$\begin{aligned}
C_{\phi D_{s0}^*D_{s1}}^{D_{s0}^*} &= \frac{1}{6} \langle s\bar{s} \rangle \left(\frac{6}{M_1^2 M_2^2} - \frac{3m_s m_c}{M_1^2 M_2^4} + \frac{3m_s^2}{M_1^4 M_2^2} + \frac{3m_c^2 m_s^2}{M_1^2 M_2^6} - \frac{3m_c^2 m_0^2}{2M_1^2 M_2^6} + \frac{3m_s^4}{M_1^4 M_2^4} - \frac{2m_0^2 m_s^2}{M_1^4 M_2^4} + \frac{3m_c^2 m_s^2}{M_1^4 M_2^4} \right. \\
&\quad \left. - \frac{2m_c^2 m_0^2}{M_1^4 M_2^4} - \frac{3q^2 m_s^2}{M_1^4 M_2^4} + \frac{2m_0^2 q^2}{M_1^4 M_2^4} - \frac{m_0^2 m_s m_c}{M_1^4 M_2^4} + \frac{3m_s^4}{M_1^6 M_2^2} - \frac{3m_0^2 m_s^2}{2M_1^6 M_2^2} \right) \times e^{-\frac{m_s^2}{M_1^2} - \frac{m_c^2}{M_2^2}}. \\
C_{\phi D_sD_s^*}^{D_s} &= \frac{1}{6} \langle s\bar{s} \rangle \left(-\frac{6}{M_1^2 M_2^2} - \frac{3m_s m_c}{M_1^2 M_2^4} - \frac{3m_s^2}{M_1^4 M_2^2} - \frac{3m_c^2 m_s^2}{M_1^2 M_2^6} + \frac{3m_c^2 m_0^2}{2M_1^2 M_2^6} - \frac{3m_s^4}{M_1^4 M_2^4} \right. \\
&\quad \left. + \frac{2m_0^2 m_s^2}{M_1^4 M_2^4} - \frac{3m_c^2 m_s^2}{M_1^4 M_2^4} + \frac{2m_c^2 m_0^2}{M_1^4 M_2^4} + \frac{3q^2 m_s^2}{M_1^4 M_2^4} - \frac{2m_0^2 q^2}{M_1^4 M_2^4} - \frac{m_0^2 m_s m_c}{M_1^4 M_2^4} - \frac{3m_s^4}{M_1^6 M_2^2} + \frac{3m_0^2 m_s^2}{2M_1^6 M_2^2} \right) \times e^{-\frac{m_s^2}{M_1^2} - \frac{m_c^2}{M_2^2}}. \\
C_{\phi D_{s0}^*D_{s1}}^\phi &= \frac{1}{6} \left\langle \frac{\alpha_s}{\pi} G^2 \right\rangle (-10\hat{I}_1(3,2,2)m_s^3 m_c^2 + 10\hat{I}_1(3,2,2)m_s^2 m_c^3 + 10\hat{I}_2(3,2,2)m_s^2 m_c^3 + 10\hat{I}_1(3,2,2)m_s m_c^4 \\
&\quad + 10\hat{I}_0^{[0,1]}(3,2,2)m_s^2 m_c - 30\hat{I}_1(3,2,1)m_s^2 m_c + 60\hat{I}_2(1,4,1)m_s^2 m_c - 20\hat{I}_2(3,2,1)m_s^2 m_c + 10\hat{I}_2^{[0,1]}(3,2,2)m_s^2 m_c \\
&\quad + 60\hat{I}_0(1,4,1)m_s^2 m_c + 10\hat{I}_1^{[0,1]}(3,2,2)m_s^2 m_c + 20\hat{I}_1(2,2,2)m_s m_c^2 + 10\hat{I}_1(3,2,1)m_s m_c^2 + 40\hat{I}_2(2,3,1)m_s m_c^2 \\
&\quad - 10\hat{I}_0(3,2,1)m_s m_c^2 - 20\hat{I}_1^{[0,1]}(3,2,2)m_s m_c^2 + 30\hat{I}_1(4,1,1)m_s m_c^2 - 10\hat{I}_2(3,2,2)m_c^5 - 10\hat{I}_0(3,2,2)m_c^5 \\
&\quad + 20\hat{I}_1(3,2,1)m_s^3 + 10\hat{I}_1(2,2,2)m_s^3 - 10\hat{I}_1(3,2,2)m_c^5 - 60\hat{I}_1(1,4,1)m_s^3 - 10\hat{I}_1^{[0,1]}(3,2,2)m_s^3 \\
&\quad - 30\hat{I}_2(4,1,1)m_c^3 + 20\hat{I}_2^{[0,1]}(3,2,2)m_c^3 + 10\hat{I}_0(3,2,1)m_c^3 - 10\hat{I}_2(3,1,2)m_c^3 - 20\hat{I}_0(2,2,2)m_c^3 \\
&\quad - 20\hat{I}_2(2,2,2)m_c^3 - 20\hat{I}_1(2,2,2)m_c^3 - 30\hat{I}_0(4,1,1)m_c^3 - 30\hat{I}_1(4,1,1)m_c^3 + 20\hat{I}_1^{[0,1]}(3,2,2)m_c^3 \\
&\quad - 10\hat{I}_0(3,1,2)m_c^3 + 20\hat{I}_0^{[0,1]}(3,2,2)m_c^3 - 50\hat{I}_1(2,2,1)m_s + 20\hat{I}_1^{[0,1]}(2,3,1)m_s - 20\hat{I}_1^{[0,1]}(3,2,1)m_s \\
&\quad + 20\hat{I}_1(1,2,2)m_s + 60\hat{I}_0(1,3,1)m_s - 20\hat{I}_2(2,2,1)m_s - 20\hat{I}_1^{[0,1]}(3,1,2)m_s - 20\hat{I}_0(2,2,1)m_s + 30\hat{I}_1(2,1,2)m_s \\
&\quad + 100\hat{I}_2(1,3,1)m_s + 10\hat{I}_1^{[0,2]}(3,2,2)m_s - 20\hat{I}_1^{[0,1]}(2,2,2)m_s + 40\hat{I}_0^{[0,1]}(2,3,1)m_s + 20\hat{I}_1(1,3,1)m_s \\
&\quad + 30\hat{I}_0(2,2,1)m_c + 30\hat{I}_2^{[0,1]}(3,1,2)m_c + 20\hat{I}_2^{[0,1]}(3,2,1)m_c + 10\hat{I}_0^{[0,1]}(3,2,1)m_c + 20\hat{I}_1^{[0,1]}(3,2,1)m_c \\
&\quad - 10\hat{I}_0^{[0,2]}(3,2,2)m_c + 20\hat{I}_1^{[0,1]}(3,1,2)m_c + 20\hat{I}_1^{[0,1]}(2,2,2)m_c + 20\hat{I}_2(2,2,1)m_c - 30\hat{I}_2(2,1,2)m_c \\
&\quad + 10\hat{I}_0(3,1,1)m_c + 20\hat{I}_0^{[0,1]}(2,2,2)m_c - 20\hat{I}_0(1,2,2)m_c - 20\hat{I}_2(1,2,2)m_c + 30\hat{I}_0^{[0,1]}(3,1,2)m_c - 10\hat{I}_1(3,1,1)m_c \\
&\quad + 20\hat{I}_2^{[0,1]}(2,2,2)m_c - 10\hat{I}_2(3,1,1)m_c - 20\hat{I}_1(2,1,2)m_c - 30\hat{I}_0(2,1,2)m_c - 10\hat{I}_2^{[0,2]}(3,2,2)m_c + 20\hat{I}_1(2,2,1)m_c \\
&\quad - 20\hat{I}_1(1,2,2)m_c - 10\hat{I}_1^{[0,2]}(3,2,2)m_c),
\end{aligned}$$

$$\begin{aligned}
C_{\phi D_s D_s^*}^\phi = & \frac{1}{6} \left\langle \frac{\alpha_s}{\pi} G^2 \right\rangle (-10\hat{I}_1(3,2,2)m_c^5 - 10\hat{I}_2(3,2,2)m_c^5 - 10\hat{I}_0(3,2,2)m_c^5 + 10\hat{I}_0(3,2,2)m_c^3 m_s^2 + 10\hat{I}_2(3,2,2)m_c^3 m_s^2 \\
& + 10\hat{I}_1(3,2,2)m_c^3 m_s^2 - 10\hat{I}_0(3,1,2)m_c^3 + 20\hat{I}_0^{[0,1]}(3,2,2)m_c^3 + 20\hat{I}_2^{[0,1]}(3,2,2)m_c^3 - 30\hat{I}_0(4,1,1)m_c^3 \\
& - 20\hat{I}_2(2,2,2)m_c^3 - 10\hat{I}_2(3,1,2)m_c^3 + 10\hat{I}_2(3,2,1)m_c^3 - 20\hat{I}_0(2,2,2)m_c^3 - 20\hat{I}_1(2,2,2)m_c^3 - 30\hat{I}_2(4,1,1)m_c^3 \\
& - 30\hat{I}_1(4,1,1)m_c^3 + 20\hat{I}_1^{[0,1]}(3,2,2)m_c^3 + 30\hat{I}_1(4,1,1)m_c^2 m_s + 20\hat{I}_1(2,2,2)m_c^2 m_s - 10\hat{I}_2(3,2,1)m_c^2 m_s \\
& + 10\hat{I}_1(3,2,1)m_c^2 m_s + 20\hat{I}_1(2,3,1)m_c^2 m_s + 40\hat{I}_0(2,3,1)m_c^2 m_s + 10\hat{I}_2^{[0,1]}(3,2,2)m_c m_s^2 + 10\hat{I}_1^{[0,1]}(3,2,2)m_c m_s^2 \\
& - 30\hat{I}_1(3,2,1)m_c m_s^2 - 20\hat{I}_0(3,2,1)m_c m_s^2 + 10\hat{I}_0^{[0,1]}(3,2,2)m_c m_s^2 + 60\hat{I}_1(1,4,1)m_c m_s^2 - 20\hat{I}_1(2,3,1)m_s^3 \\
& - 60\hat{I}_1(1,4,1)m_s^3 - 10\hat{I}_1^{[0,1]}(3,2,2)m_s^3 + 10\hat{I}_1(2,2,2)m_s^3 + 20\hat{I}_1(3,2,1)m_s^3 + 20\hat{I}_1(2,2,1)m_c \\
& + 30\hat{I}_2^{[0,1]}(3,1,2)m_c - 30\hat{I}_0(2,1,2)m_c - 20\hat{I}_1(1,2,2)m_c + 20\hat{I}_2^{[0,1]}(2,2,2)m_c - 10\hat{I}_1^{[0,2]}(3,2,2)m_c \\
& - 20\hat{I}_2(1,2,2)m_c + 20\hat{I}_1^{[0,1]}(2,2,2)m_c + 10\hat{I}_2(3,1,1)m_c - 20\hat{I}_0(1,2,2)m_c - 10\hat{I}_1(3,1,1)m_c + 20\hat{I}_1^{[0,1]}(3,2,1)m_c \\
& + 20\hat{I}_0^{[0,1]}(3,2,1)m_c + 30\hat{I}_2(2,2,1)m_c - 10\hat{I}_0^{[0,2]}(3,2,2)m_c + 20\hat{I}_0(2,2,1)m_c + 30\hat{I}_0^{[0,1]}(3,1,2)m_c \\
& - 10\hat{I}_2^{[0,2]}(3,2,2)m_c + 20\hat{I}_1^{[0,1]}(3,1,2)m_c + 20\hat{I}_0^{[0,1]}(2,2,2)m_c - 30\hat{I}_2(2,1,2)m_c - 10\hat{I}_0(3,1,1)m_c \\
& + 10\hat{I}_2^{[0,1]}(3,2,1)m_c - 20\hat{I}_1(2,1,2)m_c + 20\hat{I}_1^{[0,1]}(2,3,1)m_s + 30\hat{I}_1(2,1,2)m_s + 10\hat{I}_1^{[0,2]}(3,2,2)m_s \\
& + 40\hat{I}_2^{[0,1]}(2,3,1)m_s + 20\hat{I}_1(1,2,2)m_s - 20\hat{I}_0(2,2,1)m_s + 60\hat{I}_2(1,3,1)m_s - 20\hat{I}_1^{[0,1]}(3,2,1)m_s - 20\hat{I}_1^{[0,1]}(2,2,2)m_s \\
& + 100\hat{I}_0(1,3,1)m_s - 20\hat{I}_1^{[0,1]}(3,1,2)m_s - 50\hat{I}_1(2,2,1)m_s - 20\hat{I}_2(2,2,1)m_s + 20\hat{I}_1(1,3,1)m_s),
\end{aligned}$$

where $\langle s\bar{s} \rangle = (0.8 \pm 0.2) \langle u\bar{u} \rangle$, $\langle u\bar{u} \rangle = -(0.240 \pm 0.010)^3 \text{ GeV}^3$ at a fixed renormalization scale of about 1 GeV [32], $\langle \frac{\alpha_s}{\pi} G^2 \rangle = 0.012 \text{ GeV}^4$ [19]. Also

$$\hat{I}_l^{[m,n]}(a, b, c) = [M_1^2]^m [M_2^2]^n \frac{d^m}{d(M_1^2)^m} \frac{d^n}{d(M_2^2)^n} [M_1^2]^m [M_2^2]^n \hat{I}_l(a, b, c),$$

where \hat{I}_l ($l = 1, \dots, 3$) are defined as

$$\begin{aligned}
\hat{I}_0(a, b, c) &= \frac{(-1)^{a+b+c}}{16\pi^2 \Gamma(a)\Gamma(b)\Gamma(c)} (M_1^2)^{2-a-b} (M_2^2)^{2-a-c} U_0(a+b+c-4, 1-c-b), \\
\hat{I}_k(a, b, c) &= i \frac{(-1)^{a+b+c+1}}{16\pi^2 \Gamma(a)\Gamma(b)\Gamma(c)} (M_1^2)^{1-a-b+k} (M_2^2)^{4-a-c-k} U_0(a+b+c-5, 1-c-b),
\end{aligned}$$

where $k = 1, 2$. We can define the function $U_0(\alpha, \beta)$ as

$$U_0(a, b) = \int_0^\infty dy (y + M_1^2 + M_2^2)^a y^b \exp \left[-\frac{B_{-1}}{y} - B_0 - B_1 y \right],$$

where

$$B_{-1} = \frac{1}{M_2^2 M_1^2} (m_s^2 (M_1^2 + M_2^2)^2 - M_2^2 M_1^2 Q^2), \quad B_0 = \frac{1}{M_1^2 M_2^2} (m_s^2 + m_c^2) (M_1^2 + M_2^2), \quad B_1 = \frac{m_c^2}{M_1^2 M_2^2}.$$

- [1] M. E. Bracco, M. Chiapparini, F. S. Navarra, and M. Nielsen, *Phys. Lett. B* **605**, 326 (2005).
[2] P. Colangelo and F. De Fazio, *Phys. Lett. B* **559**, 49 (2003).
[3] Z. G. Wang, *J. Phys. G* **34**, 753 (2007).

- [4] Z. G. Wang, *Phys. Rev. D* **77**, 054024 (2008).
[5] M. E. Bracco, M. Chiapparini, F. S. Navarra, and M. Nielsen, *Phys. Lett. B* **659**, 559 (2008).
[6] F. S. Navarra, M. Nielsen, M. E. Bracco, M. Chiapparini, and C. L. Schat, *Phys. Lett. B* **489**, 319 (2000).

- [7] F. S. Navarra, M. Nielsen, and M. E. Bracco, *Phys. Rev. D* **65**, 037502 (2002).
- [8] M. E. Bracco, M. Chiapparini, A. Lozea, F. S. Navarra, and M. Nielsen, *Phys. Lett. B* **521**, 1 (2001).
- [9] B. O. Rodrigues, M. E. Bracco, M. Nielsen, and F. S. Navarra, *Nucl. Phys.* **A852**, 127 (2011).
- [10] R. D. Matheus, F. S. Navarra, M. Nielsen, and R. R. da Silva, *Phys. Lett. B* **541**, 265 (2002).
- [11] R. R. da Silva, R. D. Matheus, F. S. Navarra, and M. Nielsen, *Braz. J. Phys.* **34**, 236 (2004).
- [12] Z. G. Wang and S. L. Wan, *Phys. Rev. D* **74**, 014017 (2006).
- [13] Z. G. Wang, *Nucl. Phys.* **A796**, 61 (2007).
- [14] F. Carvalho, F. O. Durães, F. S. Navarra, and M. Nielsen, *Phys. Rev. C* **72**, 024902 (2005).
- [15] M. E. Bracco, A. J. Cerqueira, M. Chiapparini, A. Lozea, and M. Nielsen, *Phys. Lett. B* **641**, 286 (2006).
- [16] L. B. Holanda, R. S. Marques de Carvalho, and A. Mihara, *Phys. Lett. B* **644**, 232 (2007).
- [17] R. Khosravi and M. Janbazi, *Phys. Rev. D* **87**, 016003 (2013).
- [18] E. Bagan, H. G. Dosch, P. Gosdzinsky, S. Narison, and J. M. Richard, *Z. Phys. C* **64**, 57 (1994).
- [19] M. A. Shifman, A. I. Vainshtein, and V. I. Zakharov, *Nucl. Phys.* **B147**, 385 (1979).
- [20] P. Colangelo and A. Khodjamirian, in *At the Frontier of Particle Physics/Handbook of QCD*, edited by M. Shifman (World Scientific, Singapore, 2001), Vol. III, p. 1495.
- [21] V. V. Kiselev, A. K. Likhoded, and A. I. Onishchenko, *Nucl. Phys.* **B569**, 473 (2000).
- [22] J. Beringer *et al.* (Particle Data Group), *Phys. Rev. D* **86**, 010001 (2012).
- [23] I. Bediaga and M. Nielsen, *Phys. Rev. D* **68**, 036001 (2003).
- [24] P. Colangelo, F. De Fazio, and A. Ozpineci, *Phys. Rev. D* **72**, 074004 (2005).
- [25] M. Artuso *et al.* (CLEO Collaboration), *Phys. Rev. Lett.* **99**, 071802 (2007).
- [26] C. E. Thomas, *Phys. Rev. D* **73**, 054016 (2006).
- [27] Z. Guo, S. Narison, J. M. Richard, and Q. Zhao, *Phys. Rev. D* **85**, 114007 (2012).
- [28] Y. Oh, T. Song, and S. H. Lee, *Phys. Rev. C* **63**, 034901 (2001).
- [29] Z. H. Li, T. Huang, J. Z. Sun, and Z. H. Dai, *Phys. Rev. D* **65**, 076005 (2002).
- [30] F. S. Navarra, M. Nielsen, and M. R. Robilotta, *Phys. Rev. C* **64**, 021901(R) (2001).
- [31] A. Deandrea, G. Nardulli, and D. Polosa, *Phys. Rev. D* **68**, 034002 (2003).
- [32] B. L. Ioffe, *Prog. Part. Nucl. Phys.* **56**, 232 (2006).